Time-Misalignment Estimation in Overlapped DVB-S2X Waveforms

Carlos L. Marcos Rojas, †Rakesh Palisetty, Jevgenij Krivochiza, Jorge L. Gonzalez Rios, Liz Martinez Marrero, ‡Wallace Alves Martins, Juan C. Merlano Duncan, and Symeon Chatzinotas.
Interdisciplinary Centre for Security, Reliability and Trust (SnT), University of Luxembourg, Luxembourg
†*Shiv Nadar Institution of Eminence, Greater Noida , India*
‡*Institut Supérieur de l'Aéronautique et de l'Espace (ISAE-SUPAERO), Université de Toulouse, France*
Emails:(carlos.marcosrojas, jevgenij.krivochiza, jorge.gonzalez, liz.martinez-marrero, juan.duncan, symeon.chatzinotas)@uni.lu, rakesh.palisetty@snu.edu.in, wallace.martins@isae-supaero.fr

***Abstract*—Low signal strength, resulting from the distance between satellites and the Earth's surface, remains a primary challenge in integrating them into terrestrial network systems. Nevertheless, the current density of satellite constellations presents an opportunity to design cost-effective receivers capable of utilizing diversity combining techniques to overcome this issue. However, any combining technique relies heavily upon time synchronism between the received signals, which until now has presented a limitation for practical applications in satellite communication systems. This paper proposes a procedure for compensating large symbol time misalignment and estimating the remaining fractional one between two DVB-S2X waveforms (from different satellites) overlapped in time, frequency, and under noise-limited scenarios. We propose a fractional-time-misalignment estimator using the data-aided *early late gate* (ELG) principle. We evaluate the proposed estimator using the Walsh-Hadamard-based pilot sequences available in the DVB-S2X waveforms. At the same time, we present an estimation of large misalignments based on the correlation properties of the *start-of-super-frame* (SOSF) field (which uses longer Walsh-Hadamard sequences than the pilots). Simulation results show that the proposed synchronization methods provide an unbiased estimation even when the noise power levels match that of the received signals.**

***Index Terms*—Combining, Synchronization, DVB-S2X waveform, ELG, Walsh-Hadamard sequences.**

I. Introduction

The global coverage of today's satellite communication systems enables them to deliver highly reliable services at affordable costs. Integrating such systems into terrestrial networks has become a topic of great interest over the past years. Although some projects propose scenarios in which satellite communication and 5G networks could be integrated [1], challenges related to signal strength when small antennas are used and long propagation delays that hinder the synchronization process must be faced for proper integration.

As a commercial interest, small and low-cost user terminals (UTs) for medium Earth orbit (MEO), and low Earth orbit (LEO) satellite systems could benefit from the availability of several satellites in their field of view to improve the multi-connectivity diversity. Therefore, a UT may be able to leverage spatial diversity to minimize the likelihood of channel conditions leading to outages due to terrain or building shadowing. In this context, it is expected that diversity-combining techniques will be crucial in several applications, such as machine-to-machine communication, critical telecommunication setup, backhauling, and trunking.

There are numerous approaches for multi-satellite diversity, depending on the situation and system characteristics [2]–[4]. The straightforward option is the switched diversity [5], where the UT chooses one satellite out of several and creates a single link. A more sophisticated approach is the combined diversity [5], in which the UT receives the same data simultaneously through two or more satellites, improving the *signal-to-noise ratio* (SNR) of the communication link. This approach replaces challenging handover procedures with a smooth and continuous combining operation, thus boosting data throughput [5].

In a scheme where two transmission antennas are used, and only one antenna with a wide beam (capable of seeing two satellites) at the UT is employed, space-time-block-codes (STBCs), like Alamouti's code [6], present an attractive solution as a combining algorithm. However, most combining techniques rely on perfect timing synchronization [5], and in Alamouti's code, it is assumed that the symbols from different sources arrive simultaneously and in perfect alignment [6], [7]. Therefore, any misalignment between the waveforms must be compensated before any combining function is performed. However, this perfect time alignment is practically unfeasible to achieve when the position of the transmitters or the receiver constantly changes and when the signals are generated from distributed gateways (GWs) in different locations and relatively far apart [8], which is the case for *non-geostationary satellites* (NGSO). In such scenarios, the propagation channels present different time-varying conditions due to the movement of the spacecraft and/or the UT [9].

The challenges presented by the above-mentioned scenarios go beyond the capabilities of conventional multibeam satellite communication systems, where different frequencies are used for different beams. Instead, these challenges follow new trends within the satellite community where multibeam systems use adjacent spot beams with the same frequency band and polarization [10].

This work was supported by the Luxembourg National Research Fund (FNR), through the CORE Project (ARMMONY): Ground-based distributed beamforming harmonization for the integration of satellite and Terrestrial networks, under Grant FNR16352790.

In such interference-limited scenarios, conventional non-data-aided timing error detection algorithms would not perform properly and suffer from biased estimations. Therefore, a framing structure that allows synchronization under very-low *signal-to-noise-plus-interference ratio* SNIR is needed. The Digital Video Broadcasting Second Generation Extensions (DVB-S2X) standard enables data-aided synchronization algorithms by inserting known symbols in specific fields of the framing structure [11]. These fields can be used to compensate/estimate for the time difference in the arrival at the UT of the two waveforms from different satellites far apart.

Although timing synchronization methods exist for digital systems, such as Gardner's detector [12], classic early late gate (ELG) [13], and Mueller-Muller algorithm [14], none are designed to synchronize two overlapped signals in the same frequency. A similar approach to the one in this paper is proposed in [15], however, it is limited only when the misalignment between waveforms is under 3 symbols and aims to use the time-misalignment information to precompensate it at the transmitter. The main contributions of this paper are:

- A join timing-synchronization scheme between UT and GW for compensating large (i.e., integer multiples of the symbol period) time-misalignment between DVB-S2X waveforms.
- A dual timing-synchronization chain at the UT capable of locking in time two overlapped DVB-S2X waveforms and estimating the small (i.e., a fraction of the symbol period) misalignment not compensated.
- A modified ELG *timing error detection* (TED) that uses the squared of the correlation instead of the absolute values.

The paper is structured as follows. In Section II, the reference system model is presented; in Section III, the analytical design of the proposed synchronization chain at the UT is introduced; while in Section IV a scheme for two waveforms timing alignment at the GW is presented. The numerical results from simulations are discussed in section V, and finally, in section VI, the conclusions are presented.

II. System Model

In the studied scenario, we consider the forward link of a multibeam system where two satellites transmit the same data in the same frequency, using DVB-S2X waveforms with different Walsh-Hadamard sequences in the start of superframe (SOSF) and superframe-pilots (SF-P) fields. The transmitted data from the two satellites is affected by the difference in the propagation path from each satellite to the UT and the attenuation of each path. Although the difference in Doppler shift can have a significant adverse effect on the performance of the system, we relaxed such condition and assumed the receiver correctly tracks the phase and frequency of the two incoming streams, the depicted scenario is shown in Fig. 1.

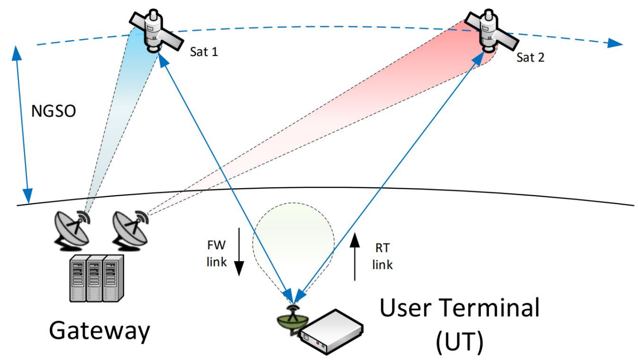

Fig. 1. Multiple satellite diversity scenario.

Then, the baseband representation of the signal received by the user is affected by a the frequency-flat Rayleigh block fading channel between the TX antennas and the user. The received signal $y(t)$ can be modeled as equation (1):

$$y(t) = x_1(t - I_1 - \tau_1) + x_2(t - I_2 - \tau_2) + w(t) \quad (1)$$

Comprising the sum of the transmitted signal $x_1(t)$ from the first satellite plus $x_2(t)$ from the second one, each signal will have different delays separated in integer (I) and fractional (τ) time-misalignment, and $w(t)$ represents an additive white Gaussian noise (AWGN).

The time-misalignment Δ between waveforms is the difference between the integer time-misalignment plus the difference between the fractional time-misalignment, i.e. equation (2).

$$\Delta = (I_1 - I_2) + (\tau_1 - \tau_2) \quad (2)$$

III. Proposed Synchronization Chain at the UT

To compensate for the integer time-misalignment, we propose that each UT in the zone where the two beams overlap calculate the distances in the number of samples between the correlation peaks of the overlapped SOSF sequences and transmit such difference back to the GW via a feedback channel from the UT to the satellite. In the GW, the average of all distances is calculated and used as the compensation value. Once the integer time-misalignment has been compensated, what remains is the fractional one that should be different for each UT and estimated individually. Fig. 2 depicts the proposed feedback scenario.

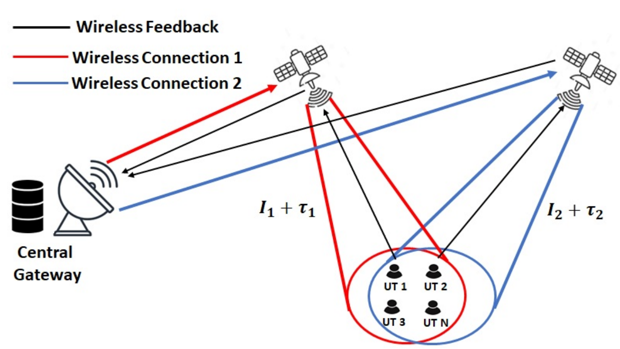

Fig. 2. Feedback scenario for multiple receivers.

When the overlapped beams' waveforms arrive at the receiver, they are down-converted and digitalized. After an initial stage of frequency acquisition and filtering after the *squared root cosine filter* (SRRC), the processing chain is separated into two branches as shown in Fig. 3, one for each beam, meaning each branch will synchronize with one of the received waveforms by advancing or delaying the signal. Forming in each branch what is known as a *delay locked loop* (DLL) [16].

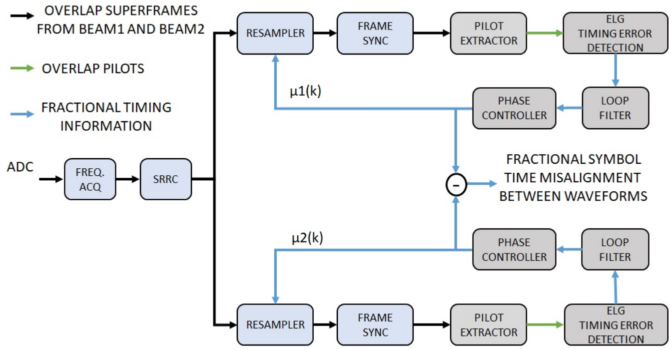

Fig. 3. Synchronization chain structure

The first stage at each separated branch is labeled as resampler, it uses information provided by the phase controller to advance or delay the waveform a fraction of the symbol time, therefore aligning the received pilots and the rest of the waveform with the receiver sample time. The resampler block is based on a Lagrangian polynomial interpolator that can estimate what an unknown sample would look like between two known samples, interpolating the input signal by a fraction μ of the sample time.

The starting point of the interpolator is that the samples $x(n)$ of the waveform contain the same information as if it were a continuous waveform $x(t)$. Therefore, a requirement for sampling base-band signals, is that the sampling period needs to be at least twice the bandwidth of the signal ($F_s \geq 2B_x$), also known as the Nyquist theorem [13]. To obtain the interpolated sample at a specific time $t_n = nT_s + \mu T_s$, the input signal $x(n)$ is convoluted with an time-variant linear filter h_I as shown in equation (3):

$$x(t_n) = \sum_{k=-2}^{2} h_I(kT_s + \mu T_s)x((n-k)T_s) \tag{3}$$

Where T_s is the sample time and μ is a real number used to calculate the filter's coefficients for each sample. Fig. 4 shows the operation of the interpolator where the blue samples represent the known samples at specific integer sample times, and the red sample is the in-between sample t_n estimated by the polynomial interpolator.

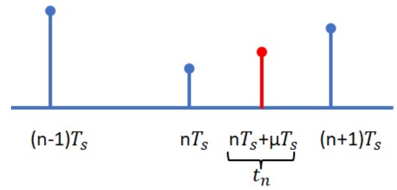

Fig. 4. Resampler Operation

The selected interpolator comprises five coefficients that can be calculated using Table I depending on the sign of μ.

TABLE I
SET OF COEFFICIENTS FOR POLYNOMIAL RESAMPLER

$h_I(n)$	$\mu < 0$	$\mu \geq 0$
$h_I(-2)$	$\frac{\mu^3-\mu}{6}$	0
$h_I(-1)$	$\frac{-\mu^3+\mu^2+2\mu}{2}$	$\frac{-\mu^3+3\mu^2-3\mu}{6}$
$h_I(0)$	$\frac{\mu^3-2\mu^2-\mu+2}{2}$	$\frac{\mu^3-2\mu^2-\mu+2}{2}$
$h_I(+1)$	$\frac{-\mu^3+3\mu^2-3\mu}{6}$	$\frac{-\mu^3+\mu^2+2\mu}{2}$
$h_I(+2)$	0	$\frac{\mu^3-\mu}{6}$

With five coefficients, such an interpolator can advance or delay the signal by a real range of two samples forward or backward [13], [17]. Therefore the values of the μ parameter provided by the phase controller can range between -2 to 2, equivalent to advancing or delaying the input signal in the range of 0.5 to -0.5 symbol time when an oversampling factor is 4. Five coefficients give an interpolation SNR of 45dB, enough for handling the SNR of the received signals.

After the resampler, the first synchronization step in each branch is performed by the frame synchronizer, whose purpose is to find a correlation peak between the incoming overlapped signals and the known SOSF Walsh-Hadamard sequence from each waveform. Once the integer symbol time misalignment between beams has been compensated, the correlation peaks in each branch should not be more than 4 samples (one symbol time) away from each other. The frame synchronizer can be implemented as a correlation filter that performs convolution between the incoming signal and the up-sampled (by a factor of 4 in our case) version of the SOSF sequence modulated in BPSK as described in [11].

Once the frame synchronizer has found the SOSF sequence in each branch, the pilot extractor counts the samples in the SF waveform and passes the ones that belong to the SF-P to the TED stage, which is the main module of the proposed design. This stage aims to estimate the error induced by the fractional symbol time offset between the waveforms and the receiver; the loop filter and phase controller use that error to calculate the value of μ to be fed into the resampler. The error is estimated in both branches of Fig. 3, where each branch produces its compensation value for the corresponding resampler.

The TED stage is based on a variation of the ELG algorithm that uses the squared instead of the absolute correlation values. It exploits the orthogonality between Walsh-Hadamard sequences and the randomization properties of the reference scrambler used in DVB-S2X to mitigate inter-pilots' interference in the overlapped waveforms. The early gate is estimated by calculating the correlation between the known pilots and the samples before the estimated position of the pilot's symbols in the waveform, while the late gate is estimated using the same procedure but with one sample after. At the same time, the correlation with the in-time samples (estimated position of the symbols) is used as a normalization factor for the error. The three correlation values are calculated using equation (4).

$$r_k(k) = \sum_{n=0}^{31} P^*{}_{known}(n) P_{received}(n-k), k = -1, 0, 1 \quad (4)$$

And the normalized error used to measure the symbol time offset is calculated using equation (5).

$$error = \frac{|r_k(1)|^2 - |r_k(-1)|^2}{|r_k(0)|^2} \quad (5)$$

The structure of the TED stage that implements equation (5) is shown in Fig. 5.

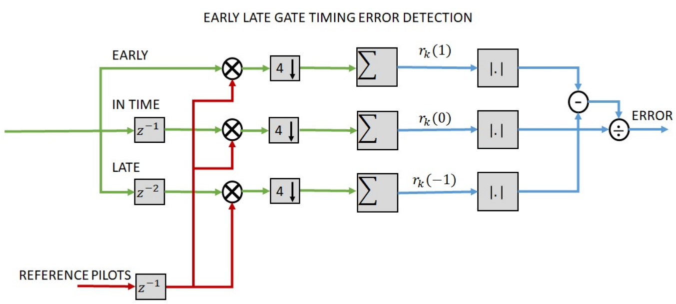

Fig. 5. Timing Error Detection

The value μ is obtained by passing the error sequence through the loop filter and the output of the loop filter through the phase controller. The selected combination for the loop filter and phase controller makes the DLL a second-order system. The structure of the filter and phase controller is shown in Fig. 6, where $e(k)$, $v(k)$ and $\mu(k)$ are the normalized error sequence, the filter output and the estimated compensation value μ respectively.

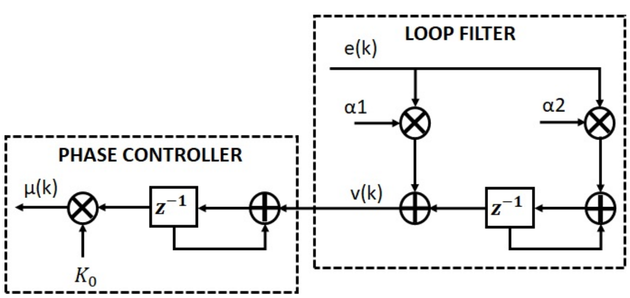

Fig. 6. Loop filter and phase controller.

The selection of the filter coefficients $\alpha1$, $\alpha2$, and the phase gain K_0 is based on a trade-off between how fast the DLL can converge to the desired value and how much variance around that value remains after the system converges. The greater the bandwidth of the filter and the larger K_0, the faster the DLL will converge, but at the same time, it will increase the variance of the estimation. On the other hand, the narrower the filter's bandwidth and the smaller K_0, it will take more time before the DLL converges, but it will do so with lower variance in the estimation. The values of the filter coefficients depend on a set of parameters standard in the design of *phase locked loops* (PLLs) but are also common in the design of DLLs. These parameters are: Noise Bandwidth (B_n), Damping Ratio (ζ), NCO Gain (K_0), and Sampling Frequency (F_s).

Once the above-mentioned parameters have been established, the filter coefficients can be calculated using equations (6) and (7).

$$\alpha_1 = \frac{1}{K_0} \frac{4\zeta}{\zeta + \frac{1}{4\zeta}} \frac{B_n}{F_s} \quad (6)$$

$$\alpha_2 = \frac{1}{K_0} \frac{4\zeta}{(\zeta + \frac{1}{4\zeta})^2} \left(\frac{B_n}{F_s}\right)^2 \quad (7)$$

With the coefficients calculated, the feedback system function in the z domain would look like equation (8).

$$\frac{\mu(z)}{e(z)} = \frac{K_0(\alpha1 z^{-1} + (\alpha2 - \alpha1) z^{-2})}{1 - 2z^{-1} + z^{-2}} \quad (8)$$

IV. Time Misalignment Compensation at the GW

At the GW, the misalignments from all the UTs are averaged, and a delay in sample time is applied to the appropriate waveform as depicted by Fig. 7.

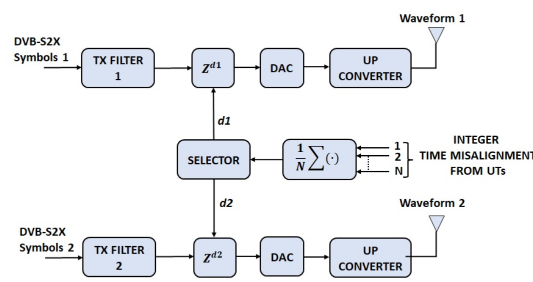

Fig. 7. GW compensation scheme.

V. Numerical Results

For simulation purposes, it was assumed that the received signal comprises two DVB-S2X waveforms with the same power. The two waveforms transmit the same data fields with different Walsh-Hadamard sequences in the SOSF and SF-P fields. As mentioned before, the first step in the synchronization chain of each branch in Fig. 3 is the detection of the SOSF sequence by the frame synchronizer; the correlation peaks detected by each frame synchronization filter are shown in Fig. 8, in this case, the distance between the peaks is 500 samples, which is to be compensated in the GW by delaying the more advanced of the two waveforms.

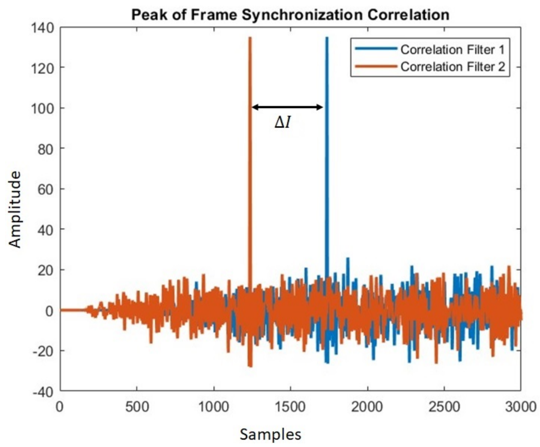

Fig. 8. SOSF detection by Frame Synchronizer.

Once the SOSF has been detected, the pilot extractor will wait for the samples of the pilot's fields and pass them to the TED module. The ELG algorithm will correlate the known pilots with the samples at the estimated position of the symbols so far, as well as one sample after (late gate) and one before (early gate).

To analyze the behavior of the TED stage when two pilot waveforms are overlapped, we computed several estimations of the three correlation values (early, late, and in-time) in the upper branch of Fig. 3. The objective of such analysis was to evaluate if noise and misalignment in the interference waveform would affect the estimation of the error function. To perform the analysis, we introduced a misalignment of 0.125 symbols to the second waveform and added AWGN to the sum of both signals. Fig. 9 shows the correlation values obtained in such conditions, and it can be noticed that even in the presence of noise and misalignment from waveform 2, the average correlation values (in red) for waveform 1 remain unchanged (fully synchronized). Therefore, the error sequence will be centered around 0, and the estimation will remain unbiased.

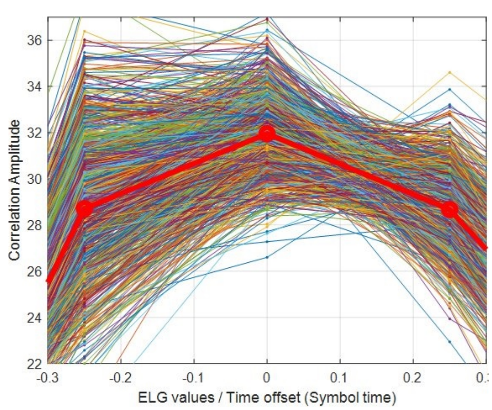

Fig. 9. Multiple correlation estimations with noise and misalignment (average value in red).

However, although misalignment between the waveforms will not affect the bias of the estimation, the loss of orthogonality between them does provoke an increment in the variance of the error function. Fig. 10 shows the variance of the error sequence for 0, 0.5, and 1 symbol time misalignment between -2 and 10 SNR. As can be seen, the lower variance in the error sequence is obtained when the waveforms are perfectly aligned.

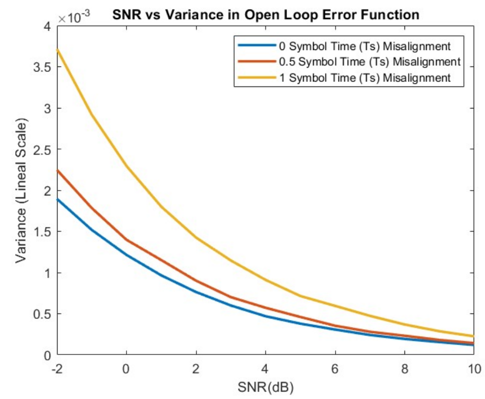

Fig. 10. Variance of the Error sequence in open loop.

The fractional time-misalignment can be estimated simply by subtracting the compensation values μ from both branches in Fig. 3. Such compensation values should converge to $-\tau_1$ in the case of μ_1 and $-\tau_2$ in the case of μ_2, so the total misalignment is calculated using equation (9).

$$\Delta\mu = -(\mu_1 - \mu_2) \tag{9}$$

The sign of $\Delta\mu$ will depend on whether waveform 1 is advanced or delayed with respect to waveform 2. Fig. 11 shows two estimations of the fractional time-misalignment for the case that $\tau_1 = 0.25$ and $\tau_2 = -0.25$ hence $\Delta\tau = 0.5$ symbol time and a noise bandwidth of $B_n = 0.75$ rad/samp in the loop filter. The blue line represents the true value of the misalignment, the yellow line shows the estimation under noiseless conditions, and the orange line shows the estimation for 0 dB SNR. It can be seen that in both cases, the estimation starts to converge around the true value near pilot 100.

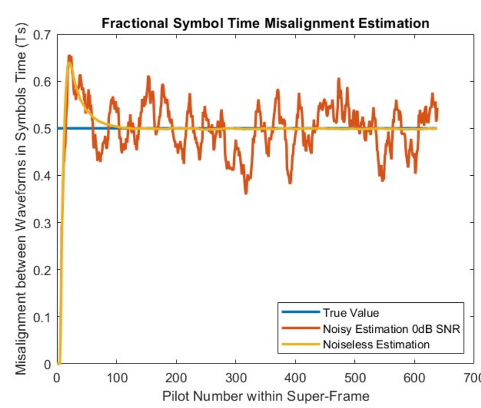

Fig. 11. Estimation of $\Delta\tau$ under noisy and perfect conditions for $B_n = 0.75$ rad/samp.

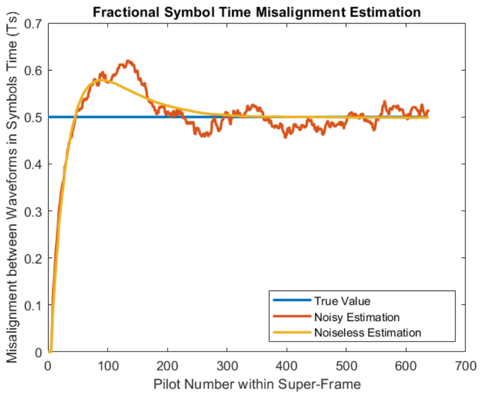

Fig. 12. Estimation of $\Delta\tau$ under noisy and perfect conditions for $B_n = 0.25$ rad/samp.

On the other hand, Fig. 12 shows the estimations for the same perfect and noisy conditions but using a bandwidth of 0.25 rad/samp in the loop filter. It is worth noting that although the SNR of the signal is the same (0 dB) as in the previous case, this estimation is less noisy than the one using 0.75 rad/samp bandwidth in the loop filter. However, because the bandwidth is one-third of the previous one, the estimations converge around the true value after pilot 300 (three times longer convergence time than before).

An analysis employing the use of different SNRs in the input signal shows that the *mean squared error* (MSE) is decreasing with increased values of the SNR (see Fig. 13).

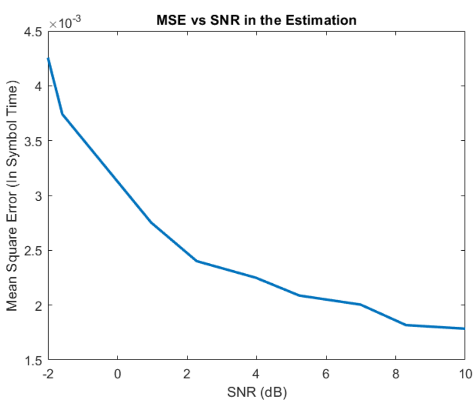

Fig. 13. Mean Squared Error of the estimation vs SNR for 0.75 B_n.

VI. Conclusions

This work presents a timing misalignment estimation and compensation procedure for overlapped DVB-S2X waveforms in multi-beam satellite combining scenarios. A simple yet robust technique, based on the large correlation peaks that can be obtained from the SOSF field, is used to detect and correct time misalignment greater than one symbol. At the same time, a modified *early late gate* TED scheme uses the SF-P to estimate the remaining fractional time-misalignment. Numerical results in open-loop and closed-loop forms showed an unbiased estimation with low variance, even in noise and interference-limited scenarios. The close loop simulation showed the importance of properly selecting the loop bandwidth and how this parameter affects the noise variance and convergence time of the estimation. Future work will include the analysis under time-variant conditions of the channel and the implementation of optimization techniques to change the loop bandwidth dynamically so that the synchronization system can track the channel changes with the lowest noise variance and convergence time in the estimation.

References

[1] K. Liolis, A. Geurtz, R. Sperber, D. Schulz, S. Watts, G. Poziopoulou, B. Evans, N. Wang, O. Vidal, B. Tiomela-Jou, M. Fitch, S.-S. Diaz, P.-S. Khodashenas, and N. Chuberr, *Satellite Communications in the 5G Era*. The Institution of Engineering and Technology, 2018, ch. 2-Satellite use cases and scenarios for 5G eMBB, pp. 25–56.

[2] D. Brennan, "Linear diversity combining techniques," *Proceedings of the IEEE*, vol. 91, no. 2, pp. 331–356, 2003.

[3] D. Skraparlis, V. K. Sakarellos, A. D. Panagopoulos, and J. D. Kanellopoulos, "Performance of n-branch receive diversity combining in correlated lognormal channels," *IEEE Communications Letters*, vol. 13, no. 7, pp. 489–491, 2009.

[4] ——, "Satellite and terrestrial diversity reception performance in tropical regions," in *2009 International Workshop on Satellite and Space Communications*, 2009, pp. 403–406.

[5] N. Mazzali, B. Shankar M., A. Rao, M. Verheecke, P. De-Cleyn, and I. De-Baere, *Satellite Communications in the 5G Era*. The Institution of Engineering and Technology, 2018, ch. 7-Diversity combining and handover techniques: enabling 5G using MEO satellites, pp. 181–207.

[6] S. Alamouti, "A simple transmit diversity technique for wireless communications," *IEEE Journal on Selected Areas in Communications*, vol. 16, no. 8, pp. 1451–1458, 1998.

[7] A. Modenini, A. Ugolini, A. Piemontese, and G. Colavolpe, "On the use of multiple satellites to improve the spectral efficiency of broadcast transmissions," *IEEE Transactions on Broadcasting*, vol. 61, no. 4, pp. 590–602, 2015.

[8] S. Kisseleff, E. Lagunas, J. Krivochiza, J. Querol, N. Maturo, L. M. Marrero, J. Merlano-Duncan, and S. Chatzinotas, "Centralized gateway concept for precoded multi-beam geo satellite networks," in *2021 IEEE 94th Vehicular Technology Conference (VTC2021-Fall)*, 2021, pp. 1–6.

[9] V. M. Baeza, E. Lagunas, H. Al-Hraishawi, and S. Chatzinotas, "An overview of channel models for ngso satellites," in *2022 IEEE 96th Vehicular Technology Conference (VTC2022-Fall)*, 2022, pp. 1–6.

[10] N. Noels, M. Moeneclaey, T. Ramírez, C. Mosquera, M. Caus, and A. Pastore, "Non-coherent rate-splitting for multibeam satellite forward link: practical coding and decoding algorithms," in *2020 IEEE 91st Vehicular Technology Conference (VTC2020-Spring)*, 2020, pp. 1–7.

[11] ETSI EN 302 307-2, "Digital Video Broadcasting (DVB); Second Generation Framing structure, Channel Coding and Modulation Systems for Broadcasting, Interactive Services, News Gathering and Other Broadband Satellite Applications; Part 2: DVB-S2 Extensions (DVB-S2X)," 2015.

[12] F. Gardner, "A bpsk/qpsk timing-error detector for sampled receivers," *IEEE Transactions on Communications*, vol. 34, no. 5, pp. 423–429, 1986.

[13] U. Mengali, *Synchronization techniques for digital receivers*, 1997th ed., ser. Applications of Communications Theory. New York, NY: Springer, Oct. 1997.

[14] K. Mueller and M. Muller, "Timing recovery in digital synchronous data receivers," *IEEE Transactions on Communications*, vol. 24, no. 5, pp. 516–531, 1976.

[15] S. Andrenacci, S. Chatzinotas, A. Vanelli-Coralli, S. Cioni, A. Ginesi, and B. Ottersten, "Exploiting orthogonality in dvb-s2x through timing pre-compensation," in *2016 8th Advanced Satellite Multimedia Systems Conference and the 14th Signal Processing for Space Communications Workshop (ASMS/SPSC)*, 2016, pp. 1–8.

[16] F. Ling and J. Proakis, *Synchronization in Digital Communication Systems*. Cambridge University Press, 2017.

[17] L. Erup, F. Gardner, and R. Harris, "Interpolation in digital modems. ii. implementation and performance," *IEEE Transactions on Communications*, vol. 41, no. 6, pp. 998–1008, 1993.